

Dual-Modality Monitoring of Tumor Response to Cyclophosphamide Therapy in Mice with Bioluminescence Imaging and Small-Animal Positron Emission Tomography

Xibo Ma, Zhaofei Liu, Xin Yang, Qiujuan Gao, Shouping Zhu, Chenghu Qin, Kai Liu, Bo Zhang, Dong Han, Fan Wang, and Jie Tian

Abstract

The purpose of this study was to noninvasively monitor the therapeutic efficacy of cyclophosphamide (CTX) in a mouse model by dual-modality molecular imaging: positron emission tomography (PET) and bioluminescence imaging (BLI). Firefly luciferase (fLuc) transfected HCC-LM3-fLuc human hepatocellular carcinoma cells were injected subcutaneously into BALB/c nude mice to establish the experimental tumor model. Two groups of HCC-LM3-fLuc tumor-bearing mice ($n = 7$ per group) were treated with saline or CTX (100 mg/kg on days 0, 2, 5, and 7). BLI and ^{18}F -fluorodeoxyglucose (^{18}F -FDG) PET scans were done to evaluate the treatment efficacy. CTX induced a $25.25 \pm 13.13\%$ and $35.91 \pm 25.85\%$ tumor growth inhibition rate on days 9 and 12 posttreatment, respectively, as determined by BLI. A good linear correlation was found between the tumor sizes measured by caliper and the BLI signals determined by optical imaging ($R^2 = .9216$). ^{18}F -FDG imaging revealed a significant uptake reduction in the tumors of the CTX-treated group compared to that in the saline control group (5.30 ± 1.97 vs $3.00 \pm 2.11\% \text{ ID/g}$) on day 16 after CTX treatment. Dual-modality molecular imaging using BLI and small-animal PET can play important roles in the process of chemotherapy and will provide noninvasive and reliable monitoring of the therapeutic response.

CYCLOPHOSPHAMIDE (CTX) is a cell cycle-dependent DNA and protein alkylating agent that has a broad spectrum of activity against a variety of neoplasms and is widely used in the clinical management of human malignancies.¹ CTX is inactive until it undergoes hepatic transformation to form 4-hydroxycyclophosphamide, which then breaks down to form the ultimate alkylating agent, phosphoramido mustard. In clinical settings, treatment of cancers by high-dose CTX is often accompanied by host cytotoxic effects, including cardiac and renal toxicity.² Therefore, a method to assess its efficacy early during treatment is needed to improve patient care. The

patients, who have no response and therefore may not benefit from the therapy, would be able to avoid unnecessary toxic side effects and switch to different, more effective therapeutic approaches in a timely manner.

Molecular imaging, the visualization, characterization, and measurement of biologic processes at the molecular and cellular levels in humans and other living systems,³ provides a noninvasive tool for early lesion detection, monitoring the therapeutic efficacy, and facilitating drug development. Thereby, it would lead to much earlier diagnosis, earlier treatment, and better prognosis, which will eventually enable personalized medicine.⁴ ^{18}F -Fluorodeoxyglucose (^{18}F -FDG)-based positron emission tomography (PET) has been well reported as a useful tool to monitor tumor responses to therapeutics. On the other hand, in vivo bioluminescence imaging (BLI) is also a sensitive imaging modality that is rapid and cost-effective and may comprise an ideal tool for early evaluation of antitumor therapies in animal models. In this study, we combined both BLI and ^{18}F -FDG microPET to investigate liver carcinoma responses to CTX treatment. It was proposed that dual BLI and small-animal PET would provide more accurate and reliable information on tumor responses to chemotherapeutics.

From the Medical Image Processing Group, Institute of Automation, Chinese Academy of Sciences, Beijing, China; Medical Isotopes Research Center, Peking University, Beijing, China; and Sino-Dutch Biomedical and Information Engineering School of Northeastern, University, Shenyang, China.

Address reprint requests to: Jie Tian, PhD, Medical Image Processing Group, Institute of Automation, Chinese Academy of Sciences, PO Box 2728, Beijing 100190, China; e-mail: jie.tian@ia.ac.cn or tian@ieee.org; or Fan Wang, PhD, Medical Isotopes Research Center, Peking University, 38# Xueyuan Road, Beijing 100191, China; e-mail: wangfan@bjmu.edu.cn.

DOI 10.2310/7290.2010.00041

© 2011 Decker Publishing

DECKER

Materials and Methods

Materials and Reagents

The cytotoxic drug CTX was obtained from Peking Union Medical College Hospital. ¹⁸F-FDG was routinely produced by the cyclotron team of the Department of Nuclear Medicine, Peking Union Medical College Hospital. The firefly luciferase (fLuc) transfected HCC-LM3 human hepatocellular carcinoma cell line^{5,6} (HCC-LM3-fLuc) was kindly provided by Prof. Jian Zhao of Shanghai Second Military Medical University.

Cell Culture and Animal Model

HCC-LM3-fLuc human hepatocellular carcinoma cells were grown in Dulbecco's Modified Eagle's Medium supplemented with 10% fetal bovine serum in a humidified incubator at 37°C in a 5% CO₂ atmosphere. Female BALB/c nude mice (4–5 weeks of age) were purchased from the Department of Experimental Animals, Peking University Health Science Center. All animal experiments were performed in accordance with the guidelines of the Institutional Animal Care and Use Committee at Peking University. The HCC-LM3-fLuc tumor model was established by subcutaneous injection of 2 × 10⁶ HCC-LM3-fLuc tumor cells into the right upper flanks of BALB/c nude mice. The mice were subjected to antitumor treatment when the tumor volume reached ≈100 mm³ (≈2 weeks after inoculation).

BLI and Image Reconstruction

All BLI experiments were performed using an *in vivo* optical molecular imaging system, ZKKS-MI-IV, which was developed by Guangzhou Zhongke Kaisheng Medical Technology Limited Company and the Molecular Imaging Research Group of the Institute of Automation, Chinese Academy of Sciences. A back-illuminated charge-coupled device (CCD) camera (1,300 × 1,340 imaging array with 20 μm pixel size, 16 bit) with a 55 mm f/2.8 lens is used to capture the bioluminescent signals. The dark current of the CCD is reduced to near-zero (0.5 electrons/pixel/hour) with liquid nitrogen cooling even for long exposures. A 12-inch integrating sphere (USS-1200V-LL Low-Light Uniform Source, Labsphere Inc., North Sutton, NH) is used to calibrate the absolute intensity in physical units of the CCD output value.

During BLI, anesthetized (2% isoflurane) animals were placed in a light-tight chamber with light-emitting diodes (LEDs) located on its top to minimize any affects of light

from outside the chamber. Photographic and bioluminescent images were acquired with LEDs on and off, respectively. The bioluminescent image was overlaid on the photographic image and represented in pseudocolor. The image acquisition and processing were performed using Windows Molecular Imaging System (WINMI) software, which was developed based on the Medical Imaging ToolKit (MITK⁷; Medical Image Processing and Analyzing Group, Institute of Automation, Chinese Academy of Sciences, Beijing, China; <www.mitk.net>). This imaging fusion technology makes it easier to discern the target tumors from the normal tissues.

In Vitro BLI

For *in vitro* BLI, a diluted series of HCC-LM3-fLuc cells were inoculated into a black 96-well plate over the range of 780 to 1 × 10⁵ cells per well (*n* = 3 per concentration). To each well was added 100 μL of a mixture of d-luciferin (Biotium, Inc., CA, Fremont) and phosphate-buffered saline solution. After incubating for 10 minutes, the plate was subjected to BLI using the ZKKS-MI-IV Imaging System (Guangzhou Zhongke Kaisheng Medical Technology Co. Ltd. and Molecular Imaging Research Group of Institute of Automation, Chinese Academy of Sciences, Guangzhou and Beijing, China). The parameters of CCD were set as f-number = 2.8, binning = 6, controller gain = 3, rate = 1 MHz, resolution = 16 bits, exposure time = 300 seconds. The optical density (OD) of the region of interest (ROI) on the grayscale image was measured by the image analysis program. The same size of ROI was selected for comparison, and the OD of the background was subtracted on each plate well.

CTX Treatment

Fourteen HCC-LM3-fLuc tumor-bearing nude mice (tumor size ≈100 mm³) were randomly divided into two groups, each of which had seven animals. In the CTX treatment group, each mouse was intraperitoneally (IP) administered with 100 mg/kg CTX in saline on days 0, 2, 5, and 7. In the control group, each animal was IP administered with saline accordingly. The tumor volume was estimated, assuming the tumors were ellipsoid, using the formula volume = 4π/3 (1/2 length × 1/2 width × 1/2 height). Tumor size and animal weight were measured every day.

In Vivo BLI

Each mouse was fasted overnight before *in vivo* BLI. The parameters of CCD were set as f-number = 2.8, binning = 4,

controller gain = 3, rate = 1 MHz, resolution = 16 bits, readout = low noise. Bioluminescent intensity was quantified from the image of peak bioluminescence using WINMI software. ROI was manually drawn over the body of the mouse. Photon-counting measurements summed bioluminescent intensity for all pixels within the ROI over the integration time.

¹⁸F-FDG MicroPET Imaging

PET scans and image analyses were performed as previously described⁸ using a microPET R4 rodent model scanner (Siemens Medical Solutions, Malvern, PA). After 16 days posttreatment, HCC-LM3-fLuc tumor-bearing nude mice were injected via the tail vein with about 3.7 MBq (100 µCi) of ¹⁸F-FDG under isoflurane anesthesia. At 1 hour postinjection, 5-minute static PET images were acquired ($n = 5$ per group). The images were reconstructed by a two-dimensional ordered-subsets expectation maximum (OSEM) algorithm, and no correction was applied for attenuation or scatter. For each microPET scan, ROI were drawn over each tumor and the contralateral background using the vendor software ASI Pro 5.2.4.0 on decay-corrected whole-body coronal images. The maximum radioactivity concentration (accumulation) within a tumor or an organ was obtained from mean pixel values within the multiple ROI volume and was converted to megabecquerels per milliliter per minute using a conversion factor. Assuming a tissue density of 1 g/mL, the ROI were converted to megabecquerels per gram per minute and then divided by the administered

activity to obtain an imaging ROI-derived percentage injected dose per gram of tissue (% ID/g).

Statistical Analysis

Quantitative data are expressed as mean \pm SD. Means were compared using one-way analysis of variance (ANOVA) and a Student *t*-test, and *p* values $< .05$ were considered statistically significant.

Results

In Vitro BLI

No significant difference between HCC-LM3 and HCC-LM3-fLuc cells was observed in terms of proliferation, tumorigenicity, or migration (data not shown). To confirm that the level of reporter gene activity is correlated with the number of cells, different numbers of HCC-LM3-fLuc cells (780 to 1×10^5) were assayed for fLuc enzyme activity. A robust linear correlation between the cell number and fLuc activity was observed ($R^2 = .9987$; Figure 1).

BLI Monitoring of the HCC-LM3 Tumor Response to CTX

Two groups of mice ($n = 7$ per group) were subjected to IP injection of either saline or CTX on days 0, 2, 5, and 7. The baseline BLI signal was determined on the fourth day before the first CTX treatment, and then BLI was done on days 0, 2, 5, 7, 9, 12, and 16, respectively, to monitor the

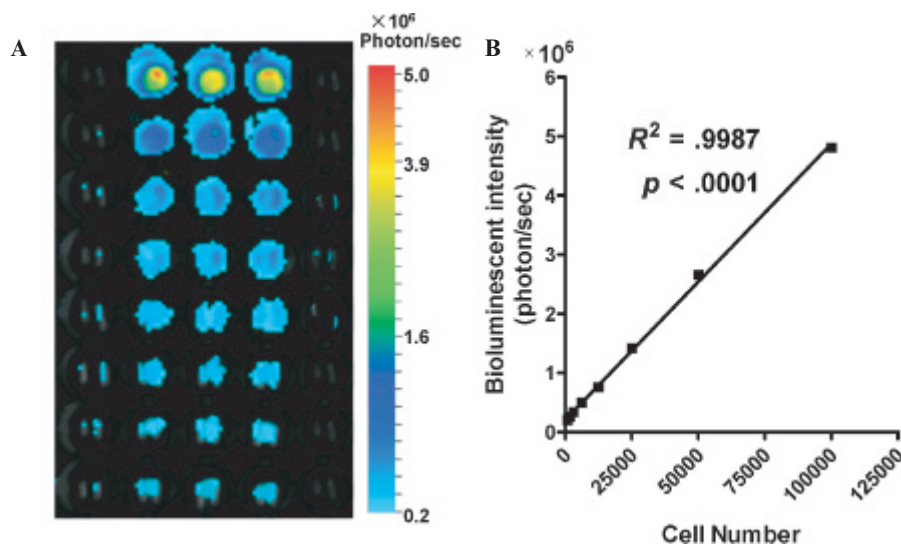


Figure 1. A, A diluted series of HCC-LM3-fLuc cells was visualized by bioluminescence imaging. A higher number of cells showed more intense bioluminescent signal. B, Correlation between the bioluminescent signals of HCC-LM3-fLuc cells and cell number. Linear regression analysis indicated high correlation between the bioluminescent signals and the cell number ($R^2 = .9987$; $p < .0001$).

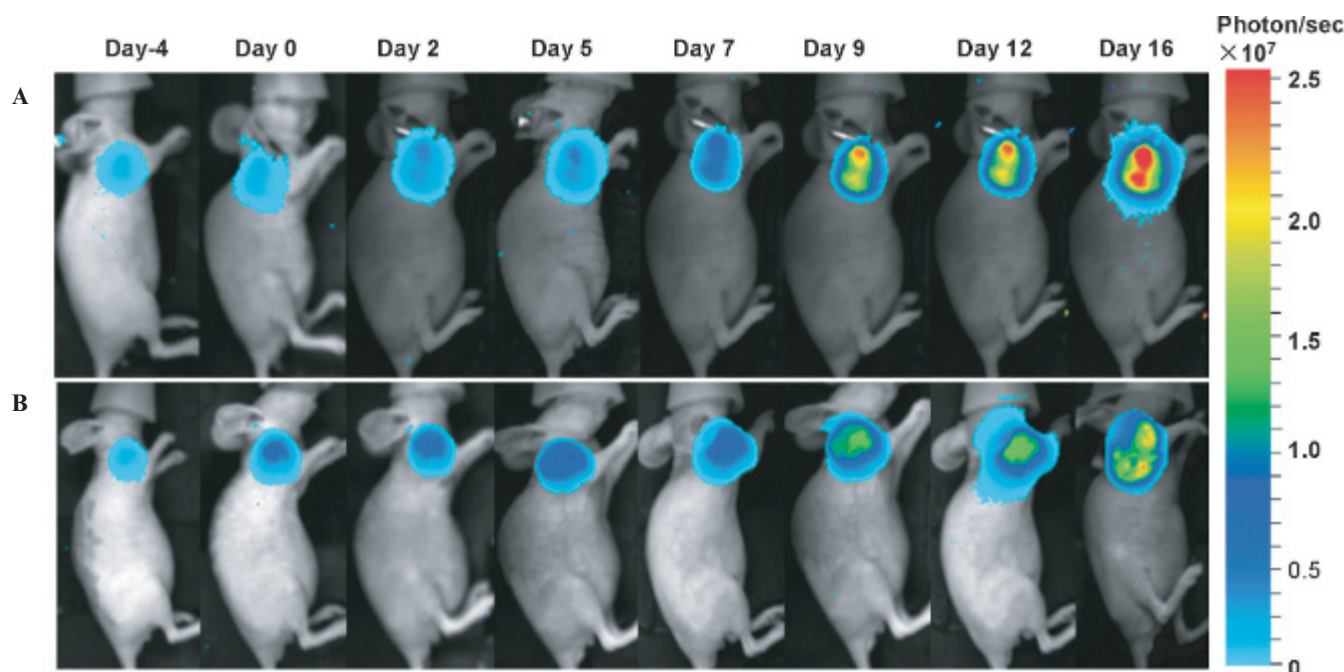


Figure 2. Serial bioluminescence images of the HCC-LM3-fLuc tumor-bearing nude mice that underwent saline (A) or cyclophosphamide (B) treatment.

progression of HCC-LM3-fLuc tumor burden. The presence of HCC-LM3-fLuc cells in the right flank could be clearly detected upon the IP injection of D-luciferin. The

BLI signals of the mice injected with saline increased exponentially and became significantly different from the CTX-treated group from day 5 onward (Figure 2 and

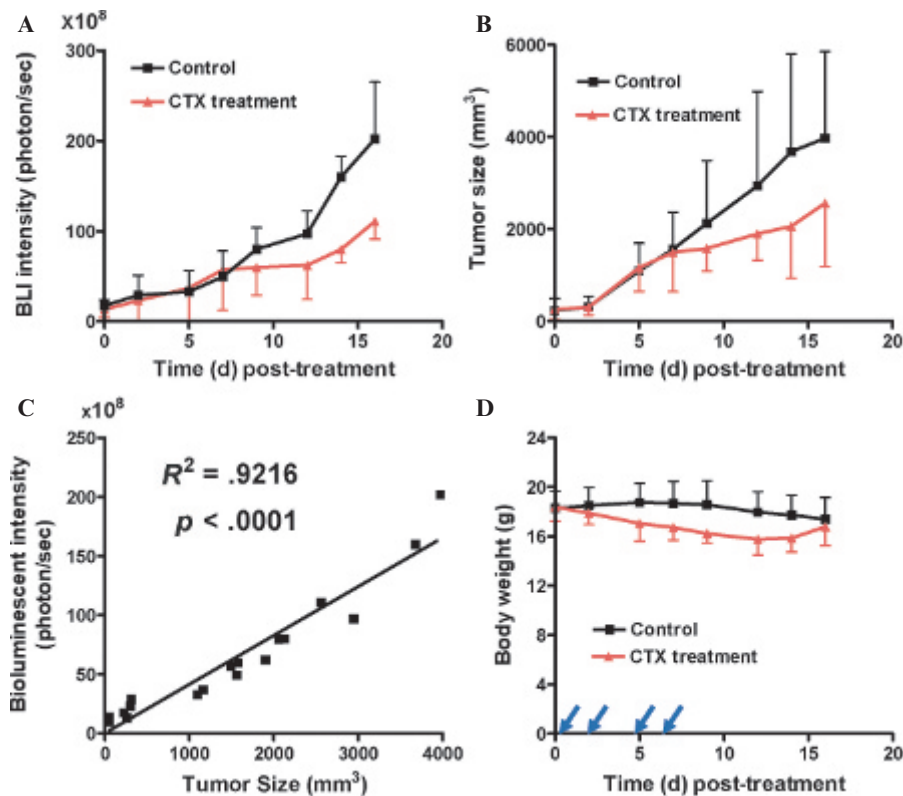


Figure 3. A, The quantified bioluminescent intensity of the HCC-LM3-fLuc tumors in the nude mice that underwent saline or cyclophosphamide (CTX) treatment. B, HCC-LM3-fLuc tumor sizes of the nude mice that underwent saline or CTX treatment. Volumes of tumors in each treatment group were measured and expressed as a function of time (mean \pm SD, $n = 7$ per group). C, Correlation between tumor bioluminescent signals measured by in vivo bioluminescence imaging and tumor sizes measured by caliper. A strong linear correlation was found ($R^2 = .9216$, $p < .0001$). D, The mice weight of the control group or the CTX-treated group over time ($n = 7$ per group). The CTX administration intervals are indicated by arrows.

Figure 3A). CTX clearly inhibited the tumor growth *in vivo*, although it was not able to completely ablate the tumor progression. We found that CTX induced a $25.25 \pm 13.13\%$ and $35.91 \pm 25.85\%$ tumor growth inhibition rate on days 9 and 12 posttreatment, respectively, as determined by BLI. The tumor sizes of nude mice were also measured by caliper. As shown in Figure 3B and 3C, the tumor sizes were increased in both groups. On day 7, the tumor size in the CTX treatment group was significantly smaller than that in the saline group. A good linear correlation was found between the tumor sizes measured by caliper and the bioluminescent signals were determined by optical imaging ($R^2 = .9216$, $p < .0001$).

Throughout the study, the weight of CTX-treated animals was monitored (Figure 3D). Although there was a slight loss of body weight from day 2 compared to the saline control group, none of the animals in the CTX-treated group lost $> 20\%$ of its original weight.

^{18}F -FDG-PET to Monitor the Treatment Efficacy of CTX

^{18}F -FDG-PET has been routinely used in both clinical and preclinical studies to evaluate the stage of tumor progression and the efficacy of therapeutic intervention by measuring the glucose metabolism. We carried out ^{18}F -FDG microPET scans on day 16 after CTX treatment. Representative decay-corrected coronal images at 1 hour after tail vein injection of ^{18}F -FDG are shown in Figure 4A. The heart had prominent uptake of ^{18}F -FDG owing to the constant beating, which has high demand for glucose. Both the saline group and the CTX-treated group had predominant ^{18}F -FDG tumor uptake compared to the contralateral background. ^{18}F -FDG imaging revealed a significant uptake reduction in the tumors of CTX-treated group compared to that in the saline control group (5.30 ± 1.97 vs $3.00 \pm 2.11\%$ ID/g; $p < .01$, Figure 4B), indicating a reduction in cell metabolic activity. To exclude the effects of the different background uptake of ^{18}F -FDG in different animals, we also calculated the tumor to background (T/B) ratios of ^{18}F -FDG at 1 hour postinjection. As shown in Figure 4C, the T/B ratios of ^{18}F -FDG in the CTX-treated group were also significantly lower than those in the saline control group ($p < .01$).

Discussion

In this study, we demonstrated the noninvasive and quantitative imaging of tumor response to CTX treatment in a mouse model using the dual-modality imaging of BLI

and small-animal PET. Many imaging techniques have been routinely used in the drug discovery process to directly monitor the drug distribution and to evaluate the effects of the drug in the context of tumor.⁹ Compared to conventional imaging modalities, molecular imaging techniques will play a pivotal role in future cancer management and personalized molecular medicine. In this study, the *in vitro* experiments showed that the activity of reporter gene was positively correlated with the number of cells, demonstrating that BLI can be used in detecting the tumor cell proliferation, namely the status of tumor

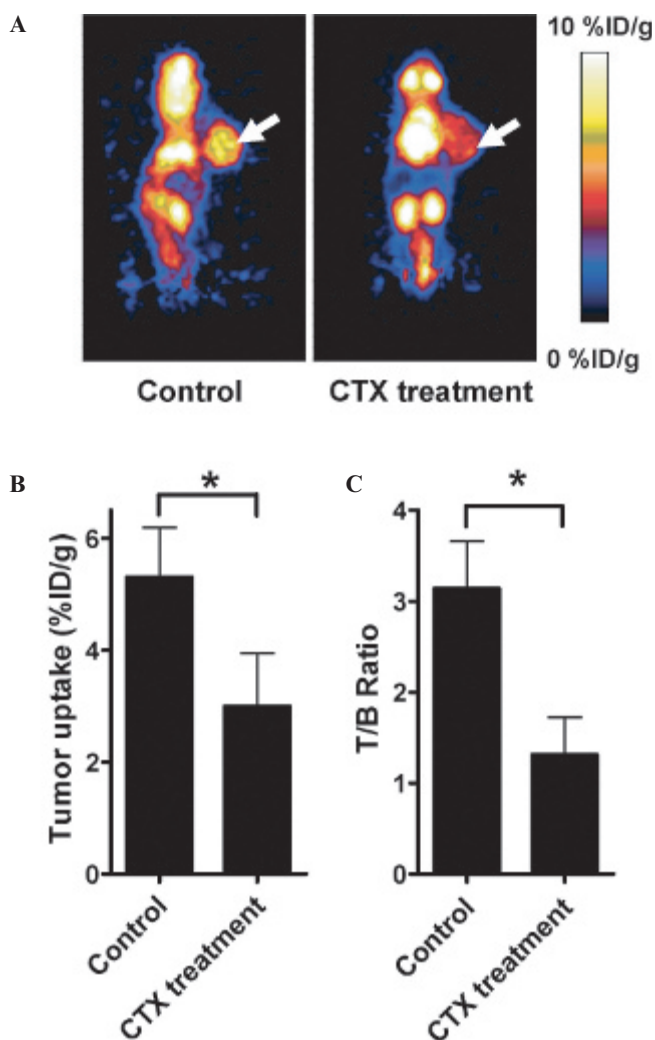


Figure 4. *A*, Representative whole-body coronal microPET images of HCC-LM3-fLuc tumor-bearing mice with ^{18}F -FDG on day 16 after cyclophosphamide (CTX) treatment. *B*, Comparison between the uptake of ^{18}F -FDG in HCC-LM3-fLuc tumors after treatment with saline or CTX. The tumor uptake values are shown as % ID/g \pm SD ($n = 5/\text{group}$). *C*, Comparison between tumor to background (T/B) ratios of ^{18}F -FDG in HCC-LM3-fLuc tumors after treatment with saline or CTX ($n = 5/\text{group}$). *indicates $p < .01$.

growth. The *in vivo* experiments showed that the intensity of the BLI was linearly correlated with the tumor volume, which was consistent with the *in vitro* result. We found that BLI and ^{18}F -FDG-PET could detect the therapeutic response of HCC-LM3-fLuc tumors to CTX treatment. For BLI, the total photon signals were significantly different between the CTX-treated group and the control group as early as day 9 after treatment. For PET, a marked reduction in ^{18}F -FDG activity in the HCC-LM3-fLuc tumors was noted for the CTX-treated group compared to the saline control group.

In vivo BLI is a sensitive imaging modality that is rapid and accessible and may comprise an ideal tool for evaluating antitumor therapies in animal models.¹⁰ Magnetic resonance imaging (MRI) was previously used to noninvasively determine the tumor size¹¹; however, both living and dead tumor cells, as well as dead tumor cell debris, infiltrating host cells, and peritumoral edema, might all contribute to the MRI-determined tumor volume. In contrast, the tumor light output of luciferase transfected tumor cells is presumably derived solely from metabolically active tumor cells. This may represent an advantage of BLI over direct measurement of tumor volume using MRI or digital caliper as it provides a quantitative surrogate measurement of the number of living tumor cells.

In conclusion, CTX therapy can inhibit the growth of hepatocellular carcinoma xenografts in the nude mouse model. Dual-modality molecular imaging using BLI and small-animal PET can play important roles in the process of the chemotherapy and will provide the noninvasive, accurate, reliable, and more statistically relevant monitoring of the therapeutic response.

Acknowledgment

Financial disclosure of authors and reviewers: None reported.

References

1. Moore MJ. Clinical pharmacokinetics of cyclophosphamide. Clin Pharmacokinet 1991;20:194–208.
2. Chen L, Waxman DJ, Chen D, Kufe DW. Sensitization of human breast cancer cells to cyclophosphamide and ifosfamide by transfer of a liver cytochrome P450 gene. Cancer Res 1996;56:1331–40.
3. Mankoff DA. A definition of molecular imaging. J Nucl Med 2007; 48:18N, 21N.
4. Cai W, Rao J, Gambhir SS, Chen X. How molecular imaging is speeding up antiangiogenic drug development. Mol Cancer Ther 2006;5:2624–33.
5. Zhao J, Dong L, Lu B, et al. Down-regulation of osteopontin suppresses growth and metastasis of hepatocellular carcinoma via induction of apoptosis. Gastroenterology 2008;135:956–68.
6. Zhao J, Lu B, Xu H, et al. Thirty-kilodalton Tat-interacting protein suppresses tumor metastasis by inhibition of osteopontin transcription in human hepatocellular carcinoma. Hepatology 2008;48: 265–75.
7. Tian J, Xue J, Dai Y, et al. A novel software platform for medical image processing and analyzing. IEEE Trans Inf Technol Biomed 2008;12:800–12.
8. Liu Z, Li ZB, Cao Q, et al. Small-animal PET of tumors with ^{64}Cu -labeled RGD-bombesin heterodimer. J Nucl Med 2009;50:1168–77.
9. Rudin M, Weissleder R. Molecular imaging in drug discovery and development. Nat Rev Drug Discov 2003;2:123–31.
10. Contag CH, Jenkins D, Contag PR, Negrin RS. Use of reporter genes for optical measurements of neoplastic disease *in vivo*. Neoplasia 2000;2:41–52.
11. Hsu AR, Cai W, Veeravagu A, et al. Multimodality molecular imaging of glioblastoma growth inhibition with vasculature-targeting fusion toxin VEGF121/rGel. J Nucl Med 2007;48:445–54.